Research Report

Real-time Variation in Number Size Distribution of Roadside Nanoparticles during One Signal Cycle

Hiroaki Minoura

Report received on May 27, 2011

ABSTRACT The behavior of nanoparticles in a roadside atmosphere has not been clarified, because nanoparticles have unstable volatile components. It is thought that the distribution of nanoparticle changes due to the variations in traffic conditions (e.g., traffic volume, velocity, and acceleration) near intersections, but the SMPS (Scanning Mobility Particle Sizer) lacks the temporal resolution required for rapid and transient measurements. Using a fast-response aerosol spectrometer capable of providing almost instantaneous measurements of particle number concentrations, the behavior of nanoparticles during one traffic signal cycle became clear. The effects of condensation and evaporation processes in addition to coagulation were shown to be important.

The relation of the number concentration in proportion to the traffic volume followed a hysteresis curve rather than a constant line during a traffic signal cycle because the gas particle equilibrium states in the roadside atmosphere were variable. Using simultaneous measurements at two points and on-board measurements, the behavior of nanoparticles was confirmed to depend on the characteristics of automotive exhaust, which vary due to the on-road driving state, engine conditions, vehicle position, or traffic light timing at an intersection. The on-board measurement of nanoparticle size distribution in the exhaust plume from a diesel vehicle was carried out as a reference for direct particle emissions and compared with the roadside nanoparticles. A coagulation/deposition model simulation using the direct particle emissions underestimated the number concentrations of the observed values. The gas/particle equilibrium model showed that the underestimated portion seemed to be caused by the condensation of ambient volatile organic compounds (VOCs) onto the particles. If this hypothesis is correct, the condensable VOC amount in the roadside atmosphere is assumed to be very large.

KEYWORDS Nanoparticle, Number Concentration, Volatile Component, Traffic, Diesel, Instrumented Junction

1. Introduction

Among the Japanese aerosol researchers and engine combustion researchers, it became the public to define nanoparticle (NP) as 50 nm or less. Furthermore, particles less than 100 nm are called ultra-fine particle (UFP). However, because the name of NP became popular in comparing with UFP, we use NP as the same definition as UFP in this study.

The behavior of NPs in the roadside atmosphere has not yet been clarified in spite of their health influence is now attracting attention. Exhaust emissions from automobiles are considered to be one of the main sources of NPs, even though the amount of particulate matter in the air has been significantly reduced through advanced automobile emission control technology. NPs show varying distributions according to season, time, and location (i.e., emission source and distance from source).

A large number of reports show that roadside number concentration (NC) distributions frequently have a peak at approximately 10–20 nm.[1-4] As one moves away from the roadside, the peak of the NC disappears rapidly and changes to the Aitken mode with a low NC. Recently, reports on the monitoring results of NC relative to the distance from the road[3,5-7] and the height from the ground[1,8] have been published to study the behavior of NPs emitted from automobiles. In selected areas around intersections, the distribution of NPs was observed by multipoint measurements.[9] On the other hand, several researchers using fixed-bed chassis dynamometer studies have reported that NCs at approximately 60–100 nm in peak diameter are the highest in diesel exhaust emissions.[10]

The size distribution of roadside NPs differs. In consideration of this difference, the relationship of the emission quality to the traffic conditions should be examined. The NC and the particle size distribution, which can be represented by the geometrical mean diameter (GMD), depend on traffic conditions such as traffic volume, velocity, or the ratio of heavy duty vehicles (HDVs). Minoura[11] measured NPs at

13 roadside sites with different traffic conditions, and the GMD showed a tendency to decrease as the percentage of HDVs increased.

Nucleation by a photochemical reaction is considered one of the processes of NP formation in urban background concentrations.[12] Even though many studies of automobile engine emission tests and roadside measurements have been conducted, few studies can explain the relationship between tailpipe NPs and roadside NPs. Not only the quantity but also the quality of automobile emissions varies with the vehicle type. To study the difference in the particle size distribution by location, occasional moving observations have been carried out.[13] On-road studies of diesel emissions in laboratory tests were reported by Kittelson et al.[14] earlier, and later by Rönkkö et al.,[15] for example. These studies showed good agreement for accumulation mode particles, and it was thought that the variation of the NC in the accumulation mode size range was simple. However, the actual behavior of NPs is difficult to understand because their behavior varies due to the traffic environment, which includes the atmospheric environment and the surroundings, such as buildings and traffic conditions. Incidentally, the scanning time of the well-known Scanning Mobility Particle Sizer (SMPS) could not keep up with the rapidly changing size distribution.

In this study, we used fast-response aerosol spectrometers instead of the SMPS and focused on the short temporal variations in the NC and the volatile components near an intersection of a busy road. Using the new device, which measures the NC distribution in real time, the NP behavior corresponding to traffic conditions changing during one traffic signal cycle could be investigated. The formation and the extinction of NPs were closely connected with semi-volatile components, and it became clear that a variation of the NCs was seen in a very short time period in the roadside atmosphere. The nucleation in the exhaust gas of diesel vehicles and the nucleation in the natural world, especially near the ground level, is beyond the scope of this study; however, Schneider et al.[16] and Iida et al.,[17] respectively, are good references for this subject. Furthermore, Enghoff and Svensmark[18] reviewed a recent nucleation study. However, as shown in Kulmala et al.,[19] a large pool of neutral clusters exist in the atmosphere, and we confirmed that these semi-volatile components (or "condensable gas") play an important role with the primary particles included in vehicle exhaust.

2. Experimental Methods

For accurate measurements, it is very important to select an area that has few elements disturbing the wind flow, such as in a street canyon. **Figure 1** shows the locations of the observation sites and the surrounding conditions in this study, and **Table 1** summarizes the measurements at each site. The details of this roadside environment, including the three-dimensional behavior of NO_x and the ozone, are

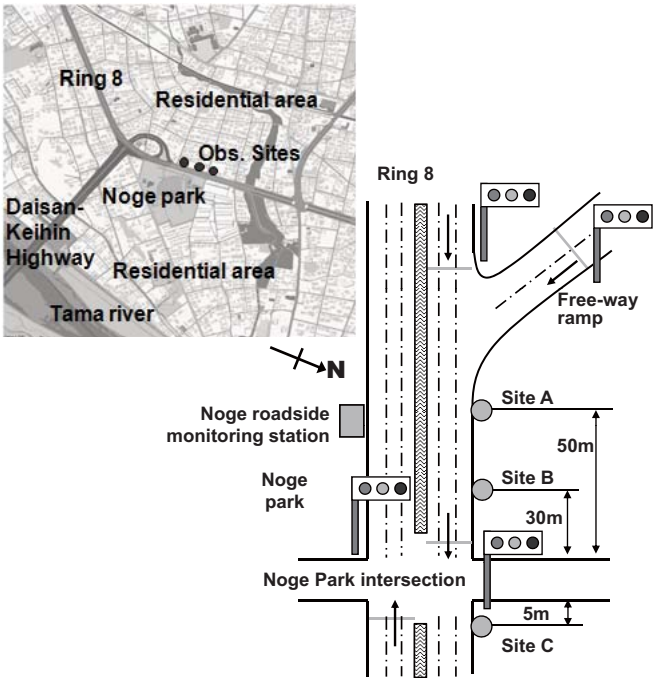

Fig. 1 Locations of the observation sites.

Table 1 Summary of roadside measurements and on-board measurements.

Measured item		Manufacture/model	Range	Data sampling
PM	number concentration	TSI Inc. USA, EEPS 3090	6.04–523.3 nm	10 Hz
	volatility	Dekati, Ltd. Finland, TD	350 °C	
Gas	NO, NO_2	Horiba Japan, APNA-360	0–1000 ± 1 ppb	1 Hz
	NH_3	Horiba Japan, APNA-360/CU-2	0–1000 ± 2% ppb	1 Hz
	CO	Horiba Japan, GA-360E	0.05–10 ppm	1 Hz
Wind	1 m height	Kaijo Japan, DA-600	0-60 ± 1% ms^{-1}	10 Hz
	3 m height	Gill USA, PREDE	0-60 ± 1.5% ms^{-1}	4 Hz
Temperature & Relative Humidity		T&D Japan, RH/TH-72S	0-50 ± 0.3°C 10-95 ± 5% RH	1 Hz
Vehicle on-board measurement	Vehicle	Toyota Japan, QuickDelivery	2.98 liter diesel engine with oxidation catalyst	
	GPS	Datatec Co. Japan, SRcomm M64	<5.2 m	1 Hz
	velocity		<±3%	10 Hz
	accelerated velocity		±2G < ±2%	10 Hz

described in Minoura and Ito.[20] Observation devices were placed near the curb of Ring 8, a large industrial road with a total of six comparably flat (< 0.1º) traffic lanes in Tokyo. The average traffic volume was 2,400 vehicles h^{-1}, and the percentage of HDVs was 11% on weekdays. The surrounding area was residential, and no large industrial facilities or factories that contribute to the air quality were present. To the south of our observation sites was Noge Park, which is more than 1 km in width and length. The north side of the observation sites had a large parking lot, and, in the surrounding areas, low-rise dwellings of less than three stories were spread out. The observation campaign was carried out in the last week of July 2005. As shown by annual data from the Noge roadside air quality monitoring station near our observation sites, a southerly wind prevails in the summer in this area. Therefore, we chose observation sites on the north side of Ring 8, where we could measure the vehicle exhaust on the road.

The three observation sites were located as follows: (A) downstream of an intersection of Ring 8 and the offramp of a highway (Daisan Keihin Highway), (B) across from Noge Park, (C) at the intersection into Noge Park. The composition of vehicle types on the two roads was different, and the percentage of HDVs coming from the highway was slightly low. The traffic volume at the observation sites was controlled by a traffic signal at the intersection at Noge Park.

As specified in Table 1, in situ continuous measurements of the NC of the NPs were acquired at the sites using two sets of Engine Exhaust Particle Sizers (EEPS; TSI, Inc., U.S.A.). The number-based size distribution of the NPs from 6.04 to 523.3 nm in diameter can be obtained with a time resolution of 10 Hz from the EEPS (Note that the EEPS used in this study was the first version of the model; the latest, Model 3090, covers 5.6 to 560 nm.). To examine the influence of the volatile components in the NPs, a thermo-denuder (TD; Dekati, Ltd., Finland), which could be heated to 350ºC, was used upstream of one of the EEPS inlets to remove these components. The three-dimensional wind direction and wind velocity were monitored by a sonic anemometer (Kaijo DA-600, Japan and Gill PREDE). A NO_x monitor (Horiba APNA-360, Japan) and an ammonia monitor (Horiba APNA-360/CU-2, Japan) using a chemical luminescence method and a CO monitor (Horiba GA-360E, Japan) using infrared absorption were used to measure air pollution gas concentrations. Ambient temperature and relative humidity were monitored by a semiconductor sensor (T&D RH/TH-72S, Japan). Because the temporal variation in the particle concentration was rapid in the roadside atmosphere, almost all devices measured with less than 1 Hz frequency. The gas monitors described above were not sufficient to follow the fast temporal variation in gas concentrations due to each vehicle outbreak (temporal response "T90" was 90 s), and so the measured gas concentrations were used for diurnal variation checking.

The devices for the measurements shown in Table 1 were installed at two places during the daytime in the observation campaign, and simultaneous measurements were carried out. During the observation campaign from July 23 to July 31, 2005, only the measurement results on July 28 and July 30 were analyzed. A southerly wind blew continuously all day on those two days, so the influence of automobile emissions could be measured on the lee side of the road. **Figure 2**

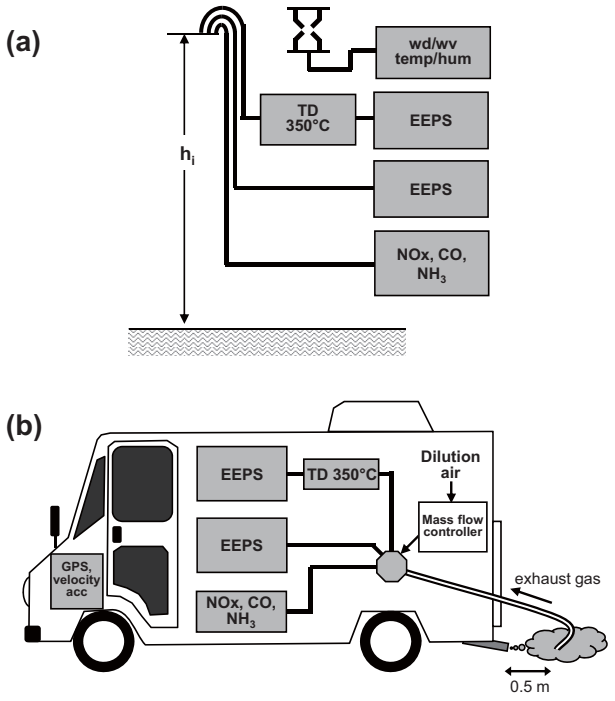

Fig. 2 Schematic view of the device configuration and sampling lines.
(a) Roadside observation: simultaneous observations at Site A and Site C at h_i = 1.5 m, observations at Site B at h_i = 1 m and 3 m simultaneously (wd/wv is wind direction/wind velocity).
(b) On-board observation: exhaust gas/particles sampled at the tailpipe rearward (0.5 m) while measuring the location and the driving state of the vehicle.

shows a schematic view of the device configuration and sampling lines. On July 28, called Run #1, the ambient air at 1 m and 3 m heights was sampled at Site B. On July 30, called Run #2, the ambient air at 1.5 m in height was sampled at Site A and Site C. The distance from the sampling lines (TSI, Inc., a conductive tube of 0.31 inch inside diameter, length < 3 m) to the measurement devices illustrated in Fig. 2(a) was set the same, and the time lag of the whole system involving the TD was measured by a short-time smoke exposure test.

Five EEPSs were prepared, and one of these five was a spare. Observations were carried out from 8:00 to 19:00, and these devices were put in a hanger built near Ring 8 at night. The differential error between the five sets of EEPSs was revised on the basis of the nano/long SMPS (TSI, Inc., 3081/3010 and 3085/3025A) data by measuring the indoor air particles in the hangar at the same time every night of the observation campaign. Including the sampling lines, the NPs in the same room were measured by the combination of the EEPS and the TD/EEPS, the same as for the roadside measurements. The TD was connected without heating. The particle size distribution distortion effect of each set (a system effect) was revised by the SMPS result. The voltage of the anode and cathode in each EEPS was identified before the observations and adjusted by cleaning the electrodes until the required value was obtained.

To examine the relationship between driving conditions and exhaust NC distribution, the same set of measuring devices was installed in a 2.98 liter diesel van, shown in Fig. 2(b), equipped with an oxidation catalyst that met the Japanese New Short Term Emission Regulation of 2003. The exhaust measurement was carried out while running at the sites. The exhaust particulate matter (PM) was sampled at a point 0.5 m rearward from the tailpipe, and continuous dilution using pure air (purity 99.9%) in a bomb and a mass flow controller (Yamatake, Japan; CMS0050) was carried out. The sulfur content in diesel fuel was previously regulated to be less than 50 ppm in Japan, and it was approximately 10 ppm in the market in 2005. The on-board measurement was carried out on July 31, and the data were used in the analyses of Run #1 and Run #2.

The traffic conditions were monitored by four sets of video cameras, and each vehicle movement was analyzed. By analyzing the video images, the type and time of every vehicle passing through in front of the measurement site was recorded.

3. Observation and Analysis

Due to the rapid changes in the NC in the roadside atmosphere caused by the exhaust PM of passing vehicles, it was very hard to observe the size distribution of the NPs correctly by using conventional devices such as the SMPS. By using the EEPS, the temporal variation in the NC distribution of the NPs could be measured even when only one vehicle passed by. In addition, a cyclic change in the NC of the NPs, which was caused by a vortex from the drag flow of the vehicle, could be observed for approximately two seconds. It became clear that a unique distribution of particles existed very locally, and it is thought that the turbulent flow on a multi-lane road makes it difficult to understand the whole distribution of the NPs in a street canyon. For example, it is very difficult to analyze the behavior of the NPs for each case when a vehicle moves in a group. Until now, research on the behavior of NPs at a roadside could only be carried out by taking temporal average values (e.g., hourly or daily) from continuous observations.

Here, the NP behavior was analyzed while taking into account the temporal variation in the traffic volume and the HDV ratio in one signal cycle at the observation location (a distance from an intersection), which has a close relation to driving conditions.

3. 1 Run #1; Variation in NPs in the Vertical Direction

3. 1. 1 Observation Results

To clarify the variation in the NPs in the vertical direction, roadside air at heights of 1 m and 3 m at Site B (Site B1 and Site B3) was measured simultaneously. The observed wind direction and wind velocity at Site B on July 28, 2005 is shown in **Fig. 3**(a), and no large variation was seen throughout the entire day. The wind direction that is perpendicular to Ring 8 is approximately 200 degrees and, as shown in Fig. 3(a), an orthogonal wind was observed at Site B1 and the daily mean wind direction was 196 degrees. At Site B3, the daily mean wind direction was 279 degrees, and the observation results could be said to be affected by traffic emission, although the wind direction deviated westerly.

The sampling point at Site B was just above a curb at Ring 8 and 30 m behind the intersection at Noge Park. The measurement equipment is shown in **Fig. 4**. The vehicles passing through at Site B were controlled by the signal at the Noge Park intersection. The cycle of this signal was 140 seconds, and the traffic volume (TV) passing by one signal was different each time. However, a big variation in the TV was not seen in Fig. 3(b), except for a slight decline at approximately noon. No traffic light cycle variation was seen during the campaign period. Passenger vehicles (petrol) contributed most to the TV, and a small declining tendency was seen in the percentage of HDVs, including buses, in the evening, but the HDV ratio was almost constant at 11%. The NC in the roadside atmosphere seemed to have the same variation as the TV variation.

As discussed above, a variation in the NPs in one signal cycle corresponding with the TV was analyzed by choosing an ideal day for stable conditions of wind variation and traffic variation. When the observed time series data were averaged every 140 seconds, which corresponded with the signal cycle, as a function of the elapsed time of the signal cycle, very smooth distributions in the TV could be obtained, as shown in **Fig. 5**(a). The time series data for 213 signal cycles

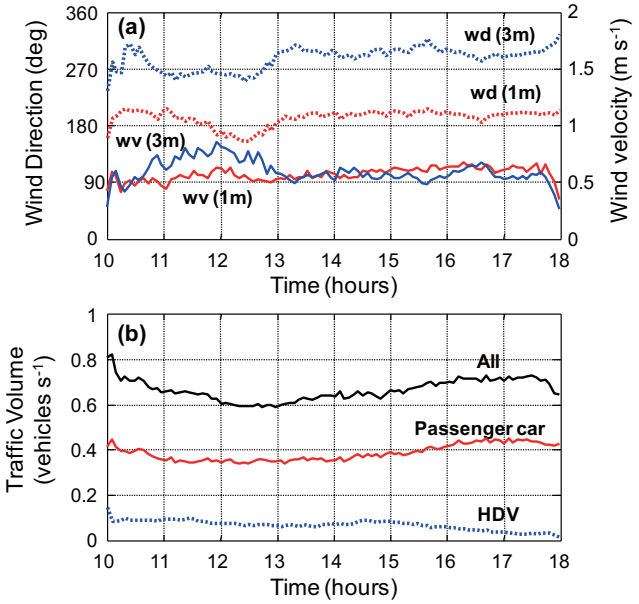

Fig. 3 Temporal variation in wind (a) and traffic volume (b) observed at Site B on July 28, 2005.

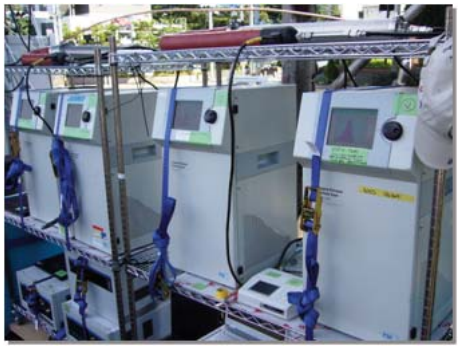

Fig. 4 Photograph of the devices measuring ambient nanoparticles of 1 m and 3 m heights at Site B.

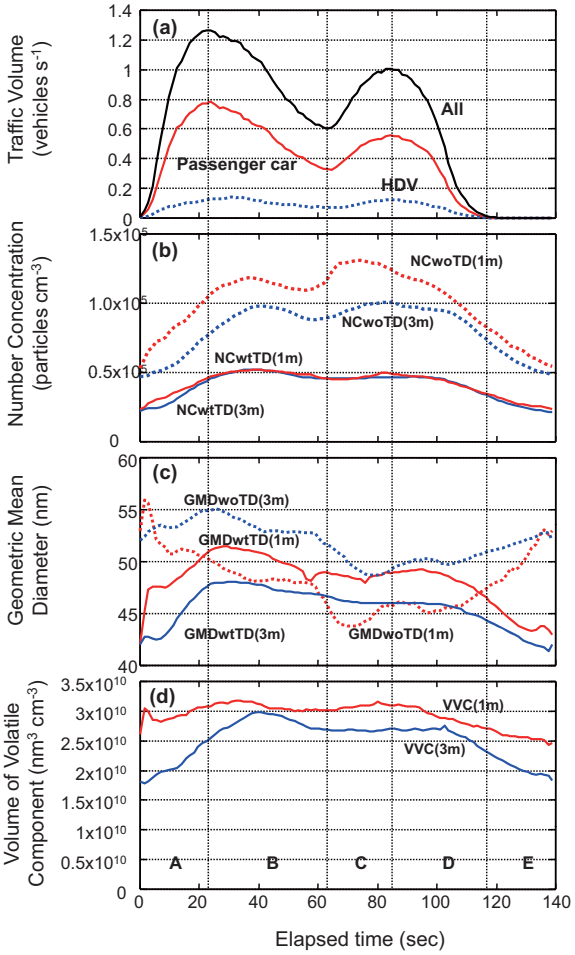

Fig. 5 Averaged values as a function of the signal elapsed time at the Noge Park intersection from data observed at Site B from 10:00 to 18:00 on July 28, 2005.
(a) Traffic volume (TV) passing through at Site B.
(b) Number concentration (NC) of ambient particles.
(c) Geometric mean diameter (GMD) of observed particles.
(d) Volume of volatile component (VVC) of observed particles, calculated from (NCwoTD – NCwtTD) on the assumption of all spherical particles.

provided from continuous observation were averaged as a function of the elapsed time of the signal in order to examine the NC and the particle size changes in one signal cycle. No variation of the cycle of the traffic signal was seen during the day.

The TV distribution had two peaks. For the first 65 seconds, the TV was dominated by vehicles from the offramp of the highway. For the next 50 seconds, the signal controlling the junction changed, and the vehicles from Ring 8 created the second TV peak. The second TV peak of all types of vehicles was small in comparison with the former peak. The averaged TV of the first peak was 0.89 vehicles s^{-1} (58.1 vehicles $cycle^{-1}$), and the averaged TV of the second peak was 0.68 vehicles s^{-1} (34.6 vehicles $cycle^{-1}$). For the last 25 seconds of the signal cycle, the traffic volume at Site B was zero because of the red light at the Noge Park intersection.

The temporal variations in the observed NC and GMD during the signal cycle were also obtained in the same way and are plotted in Figs. 5(b) and (c). The cycle variation of the NC and the GMD followed the cycle variation in the TV. Because the averaged TV was less than 1 vehicle s^{-1}, as stated above, the dispersion of the data was large. However, the averaged TV of 213 cycles showed the average vehicle passes of the observed road very well, and it is thought that the averaged NC and GMD represent the average behavior of the NPs. An increasing tendency in the NC followed the increase in the TV, and the NC without the TD treatment (NCwoTD), which involved a volatile component, showed the same variation corresponding to the two peaks of the TV distribution. The peak of the NC distributions was delayed by approximately 10 seconds relative to that of the TV peak.

The NCwoTD at the 1 m height sampling "NCwoTD(1m)" was approximately 28% higher than the NCwoTD at the 3 m height sampling "NCwoTD (3m)"; however, the NC at both heights after being treated with the TD showed the same value (NCwtTD(1m) ≈ NCwtTD(3m)). The difference values of NCwoTD is variable due to nucleation, coagulation, and condensation processes, but not for diffusion and deposition processes. However, NCwtTD includes the number concentration of non-volatile particles, such as soot particles, and the value is primarily affected by the diffusion process when we consider the difference between NCwtTD(1m) and NCwtTD(3m). This result suggests that the diffusion process can be ignored between the two height levels.

As shown in Fig. 5(c), it is clear that the GMDwtTD showed an increasing tendency following the increase in the TV. Based on this result, the vehicle emission provided comparably more non-volatile particles than those existing in the urban background. However, the temporal variation in GMDwoTD was complicated in comparison with that of GMDwtTD. A decreasing tendency in GMDwoTD(1m) was seen with an increase in NCwoTD(1m). The correlation coefficient between them was –0.72. From this, it became clear that a much greater number of smaller volatile particles (seeming to be of vehicle origin) were found compared with the NC of non-volatile particles at a height of 1 m. In contrast, GMDwoTD(3m) showed a larger value than GMDwoTD(1m), and GMDwtTD(3m) showed the opposite tendency compared to the 1 m result. That is,

GMDwoTD(1m) < GMDwtTD(1m)
GMDwoTD(3m) > GMDwtTD(3m)

during a high TV.

As shown in the relation of GMDwoTD(1m) < GMDwoTD(3m), while particles are transported from 1 m to 3 m in height, the particle size was thought to increase mainly volatile particles by coagulation, condensation, and evaporation processes. On the other hand, the deposition of non-volatile particles of bigger size was thought to occur strongly to a degree that did not affect the NC and showed the relation GMDwtTD(1m) > GMDwtTD(3m). Particle growth by the coagulation process did not seem to occur as much, based on the above discussion (NCwtTD(1m) = NCwtTD(3m)).

When the particle volume (PV) was calculated on the assumption of a spherical shape from the NC of each bin and the mobility diameter, the temporal variation in PVwoTD showed a shape close to that of NCwoTD in Fig. 5(b). The temporal variation in the volume of semi-volatile components (VVC), which is obtained by subtraction of the non-volatile components (PVwoTD – PVwtTD), is shown in Fig. 5(d).

3. 1. 2 Speculation about the Temporal Spatial Variation

The correlation coefficients for a PM parameter such as the NC and the GMD with the variation of some types of vehicles in the TV during the signal cycle are shown in **Table 2**. In total, the PV showed good correlation with the TV. Because the TV of the HDVs was much smaller than the TV of the passenger cars

(PCs), the difference by type of vehicles could not be found, and the relation with the TV of all types of vehicles is discussed. The coefficients at 3 m height for the NC and the GMD were larger than those at 1 m, but the coefficients of the PV and the VVC showed the opposite tendency. **Figure 6**(a) shows the correlation between the NCwoTD(1m) and the TV of all types of vehicles. Figure 6(b) shows the correlation between the VVC(1m) and the TV of all types of vehicles. Five symbols, A to E in Fig. 6, correspond to the data obtained for the time period shown in Fig. 5. During the elapsed time of the signal proceeding from A to E, a hysteresis shape is seen in Fig. 6(a). A difference was found in the tendency between the increasing tendency of the NC seen in A when the TV increased at the first time during the signal cycle and the decreasing tendency of the NC seen in D when the TV decreased at the last time. This means that the atmospheric condition was different between the beginning and the end because not only diffusion but also nucleation, coagulation, deposition, etc. are functions of time. As for the NCwoTD(3m) and the scatter plot of the TV, the tendency of the hysteresis was smaller than that in Fig. 6(a). On the other hand, the correlation with VVC(1m) was comparatively good, and this means that vehicle emission directly affects the VVC of the particles. However, we should consider that more than 2.5×10^{10} nm^3cm^{-3} of VVC existed in the background.

Table 2 Correlation coefficients between particle parameters and traffic volumes during the signal cycle at Site B.

			All types	PC	HDV
NC	B (1 m)	*woTD*	0.40	0.34	0.47
		wtTD	0.02	0.08	−0.07
	B (3 m)	*woTD*	0.54	0.51	0.61
		wtTD	0.54	0.56	0.54
GMD	B (1 m)	*woTD*	0.20	0.15	0.35
		wtTD	0.32	0.38	0.18
	B (3 m)	*woTD*	0.43	0.41	0.51
		wtTD	0.59	0.60	0.57
PV	B (1 m)	*woTD*	0.66	0.64	0.68
		wtTD	0.66	0.66	0.68
	B (3 m)	*woTD*	0.37	0.34	0.46
		wtTD	0.56	0.55	0.59
VVC	B (1 m)		0.50	0.46	0.50
	B (3 m)		0.26	0.23	0.38

One box simulation was carried out to examine the temporal variation in the NC shown in Fig. 5(b). The on-board measurement shown in Fig. 2(b) was carried out near Site B, and the NC distribution of the direct particle emission was analyzed as a function of vehicle velocity and vehicle acceleration on the basis of passing 31 times. **Figure 7** shows one example of the temporal variation of the number size distributions. When the target vehicle with an installed on-board measuring instrument passed just in front of Site B by the timing (i) shown in Fig. 7, the vehicle emission was observed in Site B by the timing (ii), approximately two seconds later. The mean wind speed at this time was 1.6 m sec^{-1} and Site B was located leeward. The

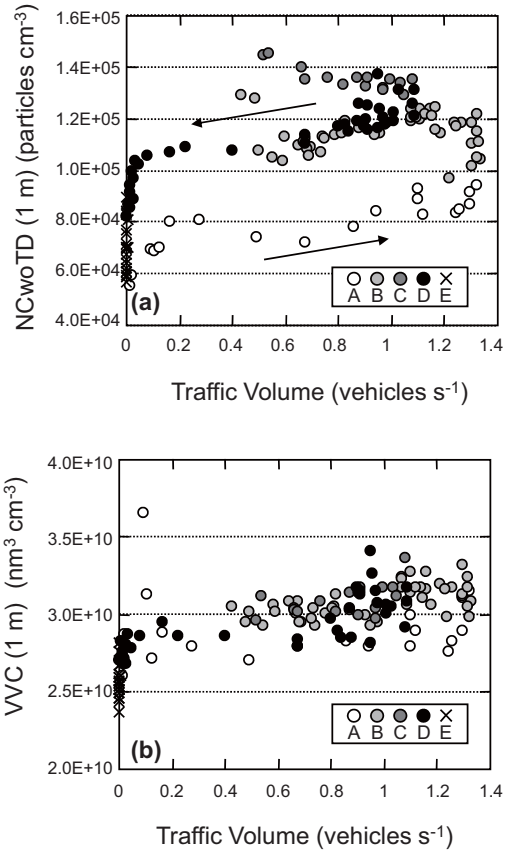

Fig. 6 Traffic volume and correlation with NC (a) and correlation with VVC (b); the relation was derived from the data shown in Fig. 4. "A" is the data between the time of zero signal elapsed time to the first peak of the TV (t = 22 s). "B" is the data between the first peak of the TV to the first valley of the TV (t = 65 s). "C" is the data between the first valley of the TV and the second peak of the TV (t = 83 s). "D" is the data between the second peak of the TV to the time of a stop signal (t = 115 s). "E" is the data during a stop signal.

highly concentrated status of the exhaust gas of the vehicle continued for approximately six seconds. A large temporal variation was not seen in the number size distribution of the vehicle emission during this highly concentrated period. The difference between the NC with the TD and the NC without the TD of the exhaust emission was small; however, a large difference of nearly 8-fold was seen in the ambient results.

With the Paramics micro-traffic model (developed by the University of Edinburgh; http://www.paramics-online.com), the traffic flow on Ring 8 was calculated, and an average vehicle velocity of 9.5 m s^{-1} and an average vehicle acceleration of 0.08 m s^{-2} at Site B was obtained. These details will be discussed later. We chose the direct particle emission of the operational status, for which the velocity and acceleration were very close. It was assumed that the NC distribution provided by the above was representative of the vehicle emission of this road and the NC was proportional to the TV, and so they were used as the temporal variation in the input data of the one box simulation as a function of the signal elapsed time. Furthermore, the observation results of the NC of the zero signal elapsed time, when the TV was zero, was used as the background concentration.

The simulated results of the coagulation deposition model in comparison with the observed results are shown in **Fig. 8**(a). The temporal variation in the NC was calculated by using the coagulation deposition model shown below in Eq. (1).[21]

$$\frac{dN_k(t)}{dt} = \frac{1}{2}\sum_{j=1}^{k-1} K_{j,k-j} N_j N_{k-j} - N_k \sum_{j=1}^{\infty} K_{k,j} N_j + S_k - R_k \quad \cdots\cdots\cdots\cdots\cdots (1)$$

The Fuchs Form of the Brownian coagulation coefficient K_{ij} is shown in the next equation.

$$K_{ij} = 2\pi (D_i + D_j)(Dp_i + Dp_j) \left(\frac{Dp_i + Dp_j}{Dp_i + Dp_j + 2(g_i^2 + g_j^2)^{1/2}} + \frac{8(D_i + D_j)}{(\bar{c}_i^{-2} + \bar{c}_j^{-2})^{1/2}(Dp_i + Dp_j)} \right)^{-1} \quad \cdots\cdots\cdots\cdots\cdots (2)$$

where $i = 1$ and $j = 2$, and

$$Kn_i = \frac{2\lambda_{air}}{Dp_i} \quad \cdots\cdots\cdots\cdots\cdots\cdots\cdots\cdots\cdots (3)$$

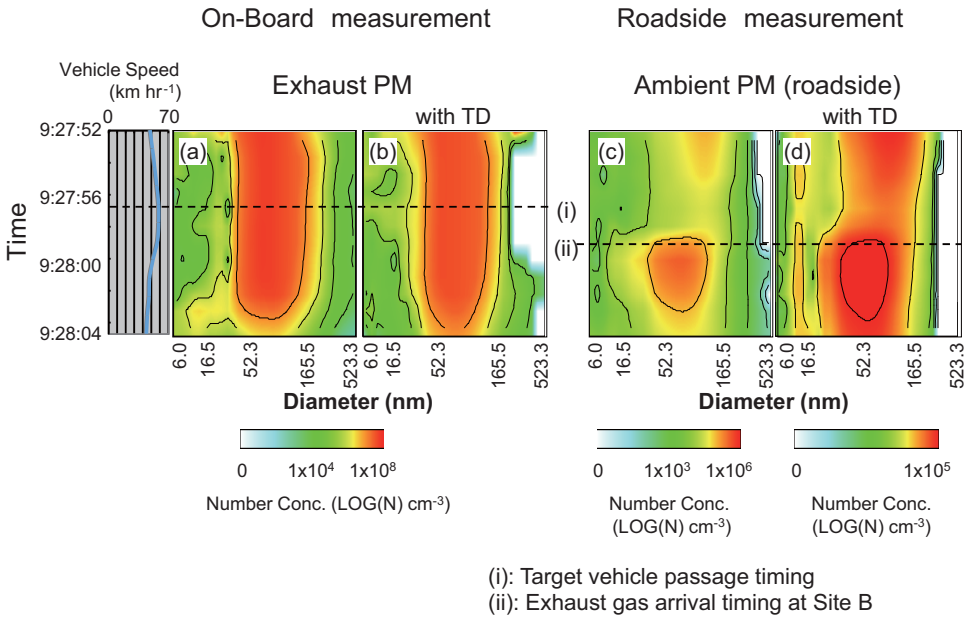

Fig. 7 Influence of the exhaust emission of the automobile on the roadside number size distribution (a comparison of the temporal variation of the number size distribution).
(a) Temporal variation of number size distribution of the automobile emission.
(b) Temporal variation of number size distribution of the automobile emission after having passed the TD.
(c) Temporal variation of number size distribution of the ambient air at Site B.
(d) Temporal variation of the number size distribution of the ambient air at Site B after having passed the TD.

$$\bar{c}_i = \left(\frac{8kT}{\pi m_i} \right)^{1/2} \quad \cdots\cdots\cdots\cdots\cdots\cdots\cdots\cdots (4)$$

$$l_i = \frac{8D_i}{\pi \bar{c}_i} \quad \cdots\cdots\cdots\cdots\cdots\cdots\cdots\cdots (5)$$

$$g_i = \frac{1}{3Dp_i l_i}\left[(Dp_i + l_i)^3 - (Dp_i^2 + l_i^2)^{3/2} \right] - Dp_i \quad \cdots (6)$$

$$D_i = \frac{kT}{3\pi\mu Dp_i}\left(\frac{5 + 4Kn_i + 6Kn_i^2 + 18Kn_i^3}{5 - Kn_i + (8+\pi)Kn_i^2} \right) \quad \cdots\cdots (7)$$

Here, m is the particle mass and Dp is the particle diameter. The NC distribution was considered as the measured Dp of 6.04 nm to 523.3 nm and was divided into 32 bins. A particle density of 1 g cm^{-3} was used, and the aerosol mean free path λ, the Boltzmann constant k, the ambient temperature T, and the viscosity coefficient μ used were 68.6 nm, 1.381×10^{-23} J K^{-1}, 293.15 K, and 1.83×10^{-4} g cm^{-1}s^{-1}, respectively. S_k is the source term and R_k is the sink (deposition) term. The observed NC distribution at signal elapsed time = 0 was given as the initial value, the exhaust PM of S_k obtained by the on-board measurement was added as a function of the TV, and the temporal variation in the NC in the box was simulated by considering the deposition process of R_k. Figure 8(a) shows the temporal variation in the non-volatile PM, and good agreement was seen for the calculated results and the observed results. In contrast, Fig. 8(b) shows the results calculated for particles including volatile components, and the simulated results compared with the observed results were underestimated.

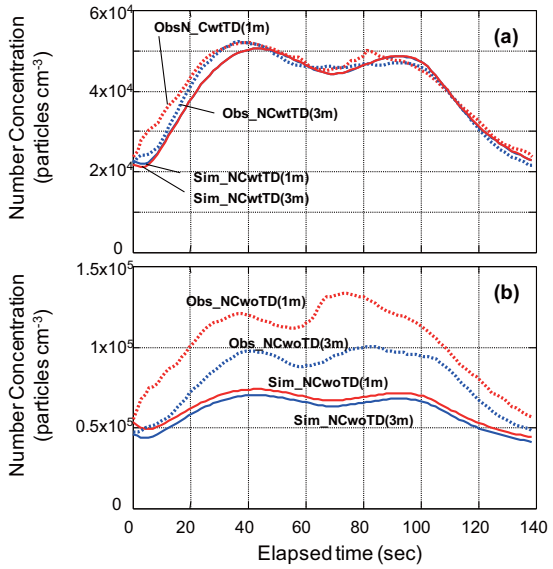

Fig. 8 Comparison of the observation data and the results of the coagulation deposition simulation.
(a) Comparison of semivolatile particles.
(b) Comparison of particles including volatile components.

We considered the exhaust PM from the on-board measurement car as representative of all types of vehicles. This might be one of the reasons for the underestimation. As another reason, nucleation and condensation processes have an effect. When a primary particle is emitted by motor vehicles, semivolatile components (also known as condensable organic compounds, "COCs") condense on the particle. The condensation process of COCs with the primary particle and the nucleated particle in the diesel exhaust were shown clearly in Schneider et al.[16] As also shown in Schneider et al.,[16] the NPs of tailpipe emission involve not only a primary particle having a solid core, such as soot, but also the particles of the volatile components without a solid core. Sulfate is one of these volatile NPs. A solid core lower than the measurement range (6.04 nm) might be involved in the tailpipe emission. Such primary particles smaller than the measurement limit could not be considered as input emission data for the box simulation. However, these small particles can become a measurable size after condensation of the COCs, and it is thought that the discrepancy in Fig. 8(b) contributed as enlarged particles. Robinson et al.[22] also mentioned the importance of COCs accompanied by condensation and nucleation processes.

The concentration of the COCs can be estimated from the difference shown in Fig. 8(b) by using the gas particle equilibrium model and assuming that the entire difference is due to the condensation process. Using the gas particle equilibrium model, we estimated the COC concentration and examined the characteristics of the variations due to time and height. **Figure 9**(a) shows the PM mass of the condensation part (PCP), which comes from the difference between the observed VVC and the simulated VVC (ObswoTD – SimwoTD), and an assumed COC density of 0.8 g cm^{-3} was used after considering that it was related with diesel fuel or petrol. According to Takekawa et al.[23] and Odum et al.,[24] the relation of PCP and COC and the

condensation efficiency (Y) is given as a function of the primary PM mass (M_o) and is defined as follows:

$$\mathrm{PCP} = Y \times \mathrm{COC} \quad \cdots\cdots\cdots\cdots\cdots\cdots\cdots\cdots (8)$$

$$Y = \frac{\sum_i M_o \alpha_i K_{om,i}}{(1 + K_{om,i} M_o)} \quad \cdots\cdots\cdots\cdots\cdots\cdots\cdots\cdots (9)$$

where $K_{om,i}$ is the gas/particle partition constant defined as

$$K_{om,i} = K_{303,i} \frac{T}{303} \exp\left[B_i \left(\frac{1}{T} - \frac{1}{303} \right) \right] \quad \cdots\cdots (10)$$

where $K_{303,i}$ is $K_{om,i}$ at 303 K, and B_i is equal to $\Delta H_{vap,i} R^{-1}$. $\Delta H_{vap,i}$ is the enthalpy of vaporization. In this study, only the first term was considered (i = 1), and the parameters of α, K_{303}, and B were provided from a smog chamber experiment based on toluene performed by Takekawa et al.[23] By using an observed road temperature T = 308 K, α, K_{303}, and B were 0.34, 5.7 × 10^{-3} m^3 μg^{-1}, and 3700, respectively. Furthermore, M_o was calculated from the value of SimNCwtTD with a density of 2.3 g cm^{-3} to take soot into consideration.

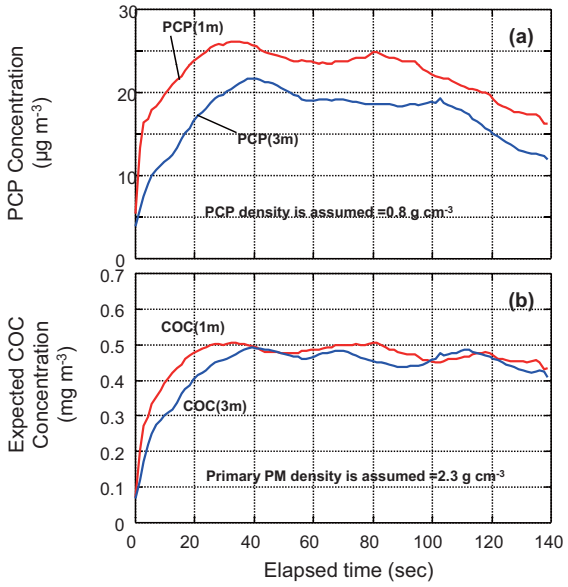

Fig. 9 Estimation of the COC by the gas particle equilibrium model.
(a) Temporal variation in the PM mass of the condensation part (PCP).
(b) Expected COC concentration originally existing in the roadside atmosphere.

Figure 9(b) shows the expected concentration of COCs at each height. From this result, if the difference shown in Fig. 8(b) is assumed to be due to the condensation of COCs, the COC concentration necessary for condensation was approximately 0.5 mg m^{-3}. Furthermore, Fig. 9(b) shows that the COC concentration did not depend on height and time, and this suggests the COCs existed uniformly in the background atmosphere. It is thought that this result is equivalent to the large pool of neutral clusters in the atmosphere, as described by Kulmala et al.[19] From the above discussion, it is suggested that COCs play an important role in NP formation at the roadside atmosphere.

The NPs appear in the vicinity of a curb locally in a route and disappear immediately in the background. The unstable nature of these NPs is considered to be due to the condensation and evaporation processes of the COCs forming the very small primary particles larger. In other words, there are abundant COCs in the roadside atmosphere, and when the primary particles are emitted, the NPs are formed through the condensation process on the particles in proportion to the number of primary particles. Therefore, it is thought that the NPs of the route can be reduced if sulfate and very small primary particles can be reduced.

3. 2 Run #2; The Variation in NPs at Different Locations

3. 2. 1 Observation Results

To clarify the variation in the NPs at a different location, roadside air at 1.5 m height was measured simultaneously at two sites. In this study, the observation results for July 30 were analyzed. On this day, a southerly wind at a wind velocity of less than 1 m s^{-1} continued, and this was the same wind condition measured on the day of Run #1. **Figure 10**(a) shows the temporal variation in the TV measured at Site C, and Figs. 10(b), (c), and (d) show the temporal variation in the PM measured at Site A and Site C and averaged using the entire data from 8:00 to 18:00 on July 30 as a function of the elapsed signal time, as in the procedure shown for Fig. 5.

As shown in Fig. 10(b), a similar tendency was seen in the temporal variation in the NC in response to the variation in the TV. The average values of the NC, when including the volatile components at Site A

"NCwoTD(A)" and Site C "NCwoTD(C)," were approximately 8.7 × 10^4 cm^{-3} and 8.3 × 10^4 cm^{-3}, respectively. However, the NC of non-volatile particles at Site C "NCwtTD(C)" was approximately 21% higher than the NC of non-volatile particles at Site A "NCwtTD(A)". In addition, the temporal variation in NCwtTD(A) was small. In Fig. 10(c), the temporal variation in particle size observed at Site C was seen in response to the TV, but only a comparatively small tendency was seen in the values observed at Site A. Furthermore, GMDwoTD(A) was smaller than GMDwtTD(A), whereas the reverse tendency was seen in the values observed at Site C. Figure 10(d) shows the temporal variation in VVC, and the value observed at Site C showed a temporal variation in response to the TV, but the value observed at Site A did not change.

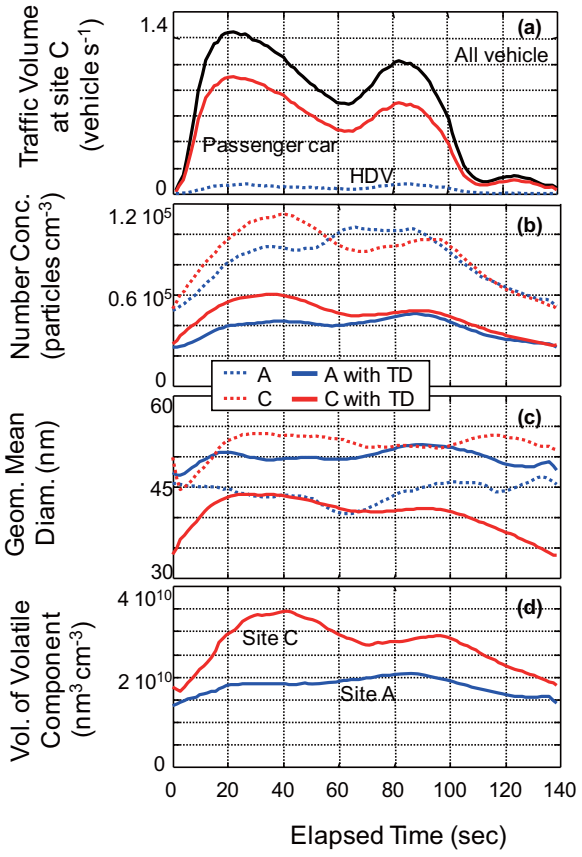

Fig. 10 Averaged values as a function of the signal elapsed time at the Noge Park intersection from the data observed at Site A and Site C from 8:00 to 18:00 on July 30, 2005.
(a) TV passing through at Site C.
(b) NC of ambient particles.
(c) GMD of the observed particles.
(d) VVC of the observed particles.

3. 2. 2 Speculation about the Influence of Different Driving States

Site A was located at the halfway point of the signal at the Noge Park intersection and the upstream signals. Most of the vehicles that passed Site A were seen running at constant velocity with little acceleration or deceleration. In contrast, Site C was located just downstream (5 m) from the Noge Park intersection. Most of the vehicles that passed Site C were observed running with acceleration. In this way, the difference in the driving states is thought to produce the difference in the NC and the GMD of the roadside particles. An increase in the NC and the GMD was clearly seen in response to the TV at the point where the vehicles were accelerating.

The traffic flow around the observation points was simulated using the Paramics micro-traffic model to evaluate the difference in the driving states quantitatively. Traffic census data and signaling information were input into this model, and every second of each vehicle location and information such as velocity and acceleration were simulated. The details of this model and the analysis results were reported by Terada et al.[25] Verification of the simulated results was compared by the temporal variation in the TV, as shown in Figs. 5(a) and 10(a), and good agreement was confirmed except for the steep increase in the TV before reaching the first peak. A simulated distribution of the velocity and the acceleration in the neighborhood of both sites is shown in **Fig. 11**. The mean vehicle velocity at both sites was approximately equal (9.1 m s^{-1} at Site A and 10.0 m s^{-1} at Site C), although the spread of the distribution was different. However, as shown in Figs. 11(c) and (d), the mean acceleration at each site is different (–0.02 m s^{-2} at Site A and 0.27 m s^{-2} at Site C), and an unbalanced distribution on the positive side is seen in Fig. 11(d). From the above evaluation, the characteristics of vehicle driving motion at each site, which were provided qualitatively from observation, could be explained quantitatively, and it became clear that the high NC involving many volatile components was observed in the area where vehicles were accelerating. The vehicle emission coefficient is used as a function of the vehicle velocity conventionally. However, the vehicle emission is different depending on whether it is cruising at the same velocity or accelerating/decelerating, even when the vehicle velocity is the same.

Next, we confirmed how many particles were present in the automobile exhaust in the acceleration state from an experiment using the on-board vehicle measurement. **Figure 12** shows the VVC distribution and the GMD distribution of the exhaust PM as a function of vehicle velocity and vehicle acceleration during 31 test drives at the sites. The VVC was calculated from the difference between NCwoTD and NCwtTD measured at the same time for each particle size on the assumption of spherical particles, as explained in the same way in Figs. 5(d) and 10(d). It became clear from Fig. 12(a) that the VVC was not present in the exhaust during deceleration, but an increasing tendency appeared with the vehicle velocity during acceleration. A similar tendency in this figure was seen in the NC distribution. This result explains that much variation was seen in the VVC at Site C with a TV in which more vehicles were accelerating, and the VVC did not change at Site A where the mean acceleration of vehicle motion was negative, as shown in Fig. 11(d). In addition, GMDwtTD showed a tendency to increase in response to the vehicle velocity in Fig. 12(b). This result means that non-volatile particles were supplied by vehicles causing GMDwtTD(C) to increase in the early phase of the signal elapsed time. The on-board vehicle used in this experiment is not representative of all vehicles but

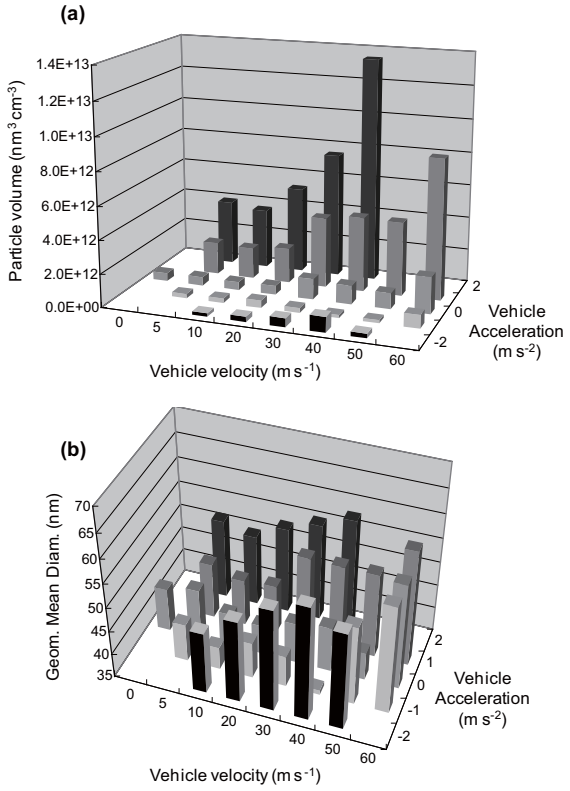

Fig. 12 Exhaust PM of on-board vehicle as a function of driving state.
(a) VVC distribution, calculated from (NCwoTD – NCwtTD) on the assumption of all spherical particles.
(b) GMDwtTD distribution.

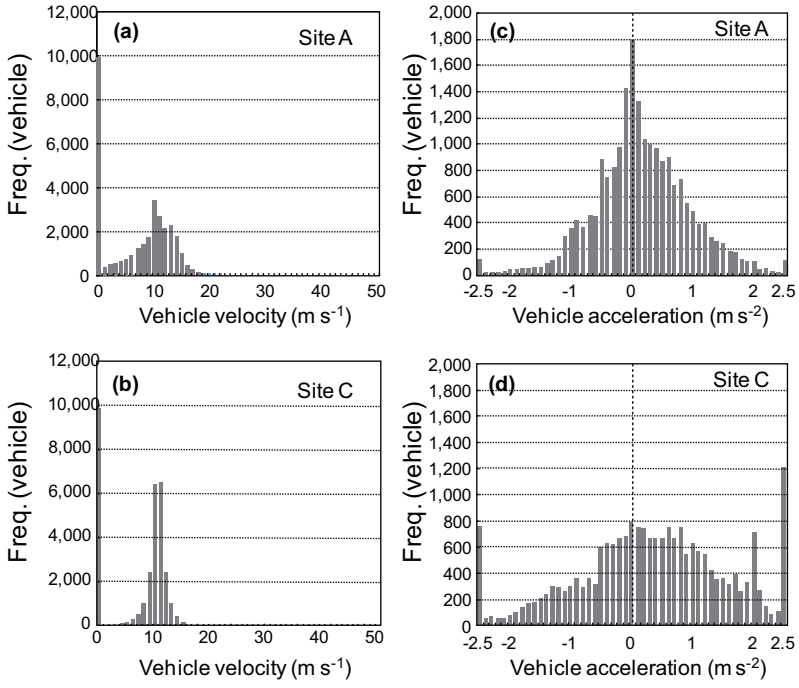

Fig. 11 Distribution of the vehicle velocity and the acceleration at Site A and Site C, simulated using the Paramix micro-traffic-flow model.

shared many of the characteristics of diesel vehicles according to the tendency shown here. Furthermore, Abdul-Khalek and Kittelson[26] suggested that even a spark ignition engine vehicle tends to be similar.

The on-board measurement results shown in Fig. 12 are different from the results obtained by a fixed bed test. Emission in the idle state or the high-load state was measured using a constant volume dilution method in the fixed bed test, under a perfect dilution condition. Whereas, a large amount of emission from a high-revolution engine state is emphasized in the roadside atmosphere or the on-board measurement results, because we observed it in a heterogeneous dilution condition. In addition to the dilution state, dilution air of approximately 50ºC was used in the fixed bed test. Furthermore, because clean air was used in the fixed bed test as the dilution air, the COC concentration involved in the roadside air was higher than the dilution air in the fixed bed test. The concept of condensation and the evaporation of COC is different by a research field, so that a difference is seen in the dilution condition and in the temperature condition. These cognitive differences have an influence on our understanding of the NPs.

4. Conclusions

1. The unstable behavior of nanoparticles in a roadside atmosphere is due to many volatile components that vary due to condensation and evaporation. During one traffic signal cycle, the variation in volatile components with the variation in traffic volume became clear for the first time.
2. The number concentration shows a correlation involving hysteresis between the traffic volume in one signal cycle because it varies according to multiple processes, not only nucleation, coagulation, and deposition, but also condensation and evaporation. However, the temporal variation in the number concentration of non-volatile particles can be explained by the variation in traffic volume with consideration of the coagulation and deposition processes.
3. A motor vehicle creates a different environment of the number concentration due to its driving state. At the site where velocity or accelerated velocity is large, the number concentration rises and the volume of semi-volatile components increases. In addition, good correlation is seen with the traffic volume and the volume of semi-volatile components.
4. The coagulation/deposition model simulation using the direct particle emissions underestimated the number concentrations compared with the observed values. The gas/particle equilibrium model could explain the underestimated portion caused by the condensation of ambient condensable organic compounds onto the particle. In a roadside atmosphere, there are many volatile particles and gases which participate in a gas-particle equilibrium. Because the number concentration of primary particles at 1 m height is greater than that at 3 m height, the volume of semi-volatile components is larger at 1 m height, but the spatial distribution of the condensable organic compounds shows no difference due to height. The condensable organic compounds are suggested to play an important role in nanoparticle formation in the roadside atmosphere.

Acknowledgements

This study was supported by the Japan Clean Air Program of the Ministry of Economy, Trade and Industry. We thank Dr. S. Kobayashi of the National Institute for Environmental Studies, Mr. N. Yanagisawa of the Isuzu Advanced Engineering Center, and Mr. H. Ito of the Toyota Motor Corporation, who leased the EEPS for this observation study.

A List of Acronyms

All (type)	all types of vehicle
COC	condensable organic compounds
EEPS	engine exhaust particle sizer, TSI's fast-response aerosol spectrometer
GMD	geometric mean diameter
GPS	Global Positioning System
hum (or RH)	relative humidity
HDV	heavy duty vehicle
NC	number concentration
NCwoTD(1m)	number concentration obtained without the thermo-denuder at 1 m height from the ground
NCwtTD(1m)	number concentration obtained with the thermo-denuder at 1 m height from the ground
NCwtTD(A)	number concentration obtained with the thermo-denuder at site A
NP	nano particle
PC	passenger car

PCP	PM mass of the condensation part
PM	particulate matter
TD	thermo-denuder
temp	atmospheric temperature
TV	traffic volume
VVC	volume of a volatile component
wd	wind direction
wv	wind velocity

References

(1) Morawska, L., Thomas, S., Gilbert, D., Greenaway, C. and Rijnders, E., "A Study of the Horizontal and Vertical Profile of Submicrometer Particles in Relation to a Busy Road", *Atmospheric Environment*, Vol.33 (1999), pp.1261-1274.

(2) Wehner, B., Birmili, W., Gnauk, T. and Wiedensohler, A., "Particle Number Size Distribution in a Street Canyon and Their Transformation into the Urban-air Background: Measurements and a Simple Model Study", *Atmospheric Environment*, Vol.36 (2002), pp.2215-2223.

(3) Zhu, Y., Hinds, W. C., Kim, S., Shen, S. and Sioutas, C., "Study of Ultrafine Particles Near a Major Highway with Heavy-duty Diesel Traffic", *Atmospheric Environment*, Vol.36 (2002), pp.4323-4335.

(4) Charron, A. and Harrison, R. M., "Primary Particle Formation from Vehicle Emissions during Exhaust Dilution in the Roadside Atmosphere", *Atmospheric Environment*, Vol.37 (2003), pp.4109-4119.

(5) Hitchins, J., Morawska, L., Wolff, R. and Gilbert, D., "Concentrations of Submicrometre Particles from Vehicle Emission Near a Major Road", *Atmospheric Environment*, Vol.34 (2000), pp.51-59.

(6) Zhang, K. M., Wexler, A. S., Zhu, Y. F., Hinds, W. C. and Sioutas, C., "Evolution of Particle Number Distribution Near Roadways. Part II: the 'Road-to Ambient' Process", *Atmospheric Environment*, Vol.38 (2004), pp.6655-6665.

(7) Kuhn, T., Biswas, S. and Sioutas, C., "Diurnal and Seasonal Characteristics of Particle Volatility and Chemical Composition in the Vicinity of a Light-duty Vehicle Freeway", *Atmospheric Environment*, Vol.39 (2005), pp.7154-7166.

(8) Ketzel, M., Wåhlin, P., Berkowicz, R. and Palmgren, F., "Particle and Trace Gas Emission under Urban Driving Conditions in Copenhagen Based on Street and Roof-level Observations", *Atmospheric Environment*, Vol.37 (2003), pp.2735-2749

(9) Minoura, H. and Takada, T., "Spatial Distribution and Size Variation of Nano/ultrafine Particle Near Busy Roadway", *Proceedings of the European Aerosol Conference*, (2005), p.271, Ghent, Belgium.

(10) Ntziachristos, L. and Samaras, Z., "Characterisation of Exhaust Particles from Diesel and Gasoline Vehicles of Different Emission Control Technologies", *Proceedings of the IMechE International Conference "21st Century Emissions Technology"* C588/023/2000 (2001), pp.93-103, London, UK.

(11) Minoura, H., "Statistical Analysis of Ultrafine Particle Numbers in Various Traffic Environment -Size Distribution of Particle Numbers-", *Journal of Japan Society for Atmospheric Environment C*, Vol.42 (2007), pp.118-128.

(12) Minoura, H. and Takekawa, H., "Observation of Number Concentrations of Atmospheric Aerosols and Analysis of Nanoparticle Behavior at an Urban Background Area in Japan", *Atmospheric Environment*, Vol.39 (2005), pp.5806-5816.

(13) Weijers, E. P., Khlystov, A. Y., Kos, G. P. A. and Erisman, J. W., "Variability of Particulate Matter Concentrations along Roads and Motorways Determined by a Moving Measurement Unit", *Atmospheric Environment*, Vol.38 (2004), pp.2993-3002.

(14) Kittelson, D. B., Johnson, J., Watts, W., Wei, Q., Drayton, M., Paulsen, D. and Bukowiecki, N., "Diesel Aerosol Sampling in the Atmosphere", *SAE Tech. Pap. Ser.*, No.2000-01-2212 (2000).

(15) Rönkkö, T., Virtanen, A., Vaaraslahti, K., Keskinen, J., Pirjola, L. and Lappi, M., "Effect of Dilution Conditions and Driving Parameters on Nucleation Mode Particles in Diesel Exhaust: Laboratory and On-road Study", *Atmospheric Environment*, Vol.40 (2006), pp.2893-2901.

(16) Schneider, J., Hock, N., Weimer, S. and Borrmann, S., "Nucleation Particles in Diesel Exhaust: Composition Inferred from In Situ Mass Spectrometric Analysis", *Environmental Science and Technology*, Vol.39 (2005), pp.6153-6161.

(17) Iida, K., Stolzenburg, M., McMurry, P., Dunn, M. J., Smith, J. N., Eisele, F. and Keady, P., "Contribution of Ion-induced Nucleation to New Particle Formation: Methodology and Its Application to Atmospheric Observations in Boulder, Colorado", *Journal of Geophysical Research*, Vol.111 (2006), D23201.

(18) Enghoff, M. B. and Svensmark, H., "The Role of Atmospheric Ions in Aerosol Nucleation – A Review", *Atmospheric Chemistry and Physics*, Vol.8 (2008), pp.4911-4923.

(19) Kulmala, M., Riipinen, I., Sipilä, M., Manninen, H. E., Petäjä, T., Junninen, H., Maso, M. D., Mordas, G., Mirme, A., Vana, M., Hirsikko, A., Laakso, L., Harrison, R. M., Hanson, I., Leung, C., Lehtinen, K. E. J. and Kerminen, V.-M., "Towards Direct Measurement of Atmospheric Nucleation", *Science*, Vol.318 (2007), pp.89-92.

(20) Minoura, H. and Ito, A., "Observation of the Primary NO_2 and NO Oxidation Near the Trunk Road in Tokyo", *Atmospheric Environment*, Vol.44 (2010), pp.23-29.

(21) Seinfeld, J. H. and Pandis, S. N., *Atmospheric Chemistry and Physics*, (1997), pp.1360, John Wiley and Sons Ltd.
(22) Robinson, A. L., Donahue, N. M., Shrivastava, M. K., Weitkamp, E. A., Sage, A. M., Grieshop, A. P., Lane, T. E., Pierce, J. R. and Pandis, S. N., "Rethinking Organic Aerosols: Semivolatile Emissions and Photochemical Aging", *Science*, Vol.315 (2007), pp.1259-1262.
(23) Takekawa, H., Minoura, H. and Yamazaki, S., "Temperature Dependence of Secondary Organic Aerosol Formation by Photo-oxidation of Hydrocarbons", *Atmospheric Environment*, Vol.37 (2003), pp.3413-3424.
(24) Odum, J. R., Hoffmann, T., Bowman, F., Collins, D., Flagan, R. C. and Seinfeld, J. H., "Gas/particle Partitioning and Secondary Organic Aerosol Yields", *Environmental Science and Technology*, Vol.30 (1996), pp.2580-2585.
(25) Terada, S., Tanahashi, I., Hayashi, S., Yoshikawa, Y. and Kunimi, H., "Development of Microscopic Traffic Simulation Model for Estimation of Roadside Emissions in JCAP". *Proceedings of the International Federation of Automotive Engineering Societies 2006 World Automotive Congress*, (2006), Yokohama, Japan.
(26) Abdul-Khalek, I. S. and Kittelson, D. B. "Real Time Measurement of Volatile and Solid Exhaust Particles Using a Catalytic Stripper", *SAE Tech. Pap. Ser.* No.950236 (1995).

Hiroaki Minoura
Research Field:
- Atmospheric Science
Academic Degree: Dr. Sci.
Academic Societies:
- Meteorological Society of Japan
- Japan Society for Atmospheric Environment
- Japan Association of Aerosol Science and Technology
Award:
- Best Poster Presentation Award on Harmonisation within Atmospheric Dispersion Modeling for Regulatory Purposes, 2008